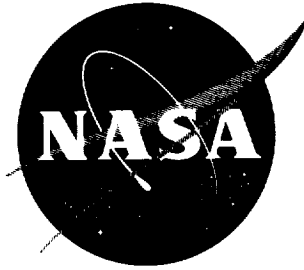


code - 1



TECHNICAL NOTE

D-1655

PREDICTION OF VELOCITY REQUIREMENTS FOR MINIMUM TIME
ABORTS FROM THE MIDCOURSE REGION
OF A LUNAR MISSION

By Robert B. Merrick and George P. Callas

Ames Research Center
Moffett Field, Calif.

NATIONAL AERONAUTICS AND SPACE ADMINISTRATION
WASHINGTON

April 1963

Code-1

CASE FILE COPY

TABLE OF CONTENTS

	<u>Page</u>
SUMMARY	1
INTRODUCTION	1
NOTATION	2
PRELIMINARY CONSIDERATIONS	4
Applicable Midcourse Regions	4
Fuel Available	5
ANALYSIS	5
The Mathematical Model	5
The Two-Body Analysis	7
Effects of Two-Body Analysis	9
Modified Two-Body Analysis	10
Error Analysis	11
RESULTS AND DISCUSSION	11
Primary Data	11
Midcourse Correction Following an Abort	13
Graphical Prediction of an Abort Maneuver	14
CONCLUSIONS	14
APPENDIX A - CONSTANCY OF ORBIT PLANE	16
APPENDIX B - MINIMUM TIME TO RETURN REQUIRES MINIMUM V_R	18
APPENDIX C - DERIVATION OF THE ABORT-VELOCITY PREDICTION EQUATION	21
APPENDIX D - OBSERVATION AND VELOCITY CORRECTION SCHEDULE USED ON OUTGOING TRAJECTORY	23
REFERENCES	24
TABLES	25
FIGURES	27

NATIONAL AERONAUTICS AND SPACE ADMINISTRATION

TECHNICAL NOTE D-1655

PREDICTION OF VELOCITY REQUIREMENTS FOR MINIMUM TIME

ABORTS FROM THE MIDCOURSE REGION

OF A LUNAR MISSION

By Robert B. Merrick and George P. Callas

SUMMARY

15052

Problems associated with quick returns to the earth from the midcourse region of a lunar mission have been examined by relating errors in perigee height to some of the errors inherent in any abort maneuver.

Abort trajectories were computed at several ranges and with various fuel capabilities on both the outgoing and incoming legs of a typical circumlunar trajectory. The representation of the physical system included the gravitational effects of the sun and the moon and the second harmonic term of the earth's oblateness, but abort rocket firings were taken as impulses.

A Keplerian trajectory was used for determining the direction of the abort rocket thrust in the orbit plane and a modification to this approach is presented which markedly reduces the altitude error, at perigee, due to the two-body approximation of the four-body physical system. This modification is based on a reference trajectory concept.

Four sources of error, other than the two-body approximation effects, were considered and their influence upon the perigee height at return was examined statistically. These error sources are the inaccuracy in the knowledge of position and velocity at abort and the inaccuracies in the magnitude and aiming of the abort rocket. The aiming error in the thrust applied during abort was responsible for major perigee deviations.

The velocity increments necessary to correct the errors incurred by the abort maneuver were computed at various points on the return trajectory. Less than 5 percent of the abort velocity increment is sufficient to correct these errors if the correction is applied at a range of 100,000 km from the earth.

INTRODUCTION

A substantial effort has been devoted to analyzing abort procedures for the launch phase of flight of a manned spacecraft but, aside from the work of Kelly

and Adornato (ref. 1) and Miller and Deyst (ref. 2), little work has been done on the capabilities and requirements of midcourse aborts.

There appears to be little possibility that an abort system designed for launch conditions would be suitable for midcourse abort since the requirements for speed of execution and aiming accuracy have opposite emphasis. The launch abort must be executed immediately, must have very high thrust because of the importance of time, but requires only moderate aiming accuracy (ref. 3), whereas the midcourse abort has less need for speed of execution but requires maximum aiming accuracy.

The precise determination of the direction of the rocket thrust in midcourse aborts would be straightforward if the gravitational attractions of the sun and moon were of negligible consequence in earth-moon space. Since these gravitational attractions do have considerable effect, it is highly desirable that the prediction of the abort velocity allow for these forces in some fashion.

This report is devoted to the minimum return time abort in which time is all important and the selection of a landing site is secondary. This type of abort would be used when the quickest possible entry into the atmosphere was desired, for example, in the event of a crack in the cabin wall, or of an impending major radiation storm. The minimum time return also provides a basis for evaluating the return time penalty associated with selection of a landing site. Aborts for which return time is not a primary factor are not considered herein.

This report presents the details of an abort navigation system which determines the trajectory that returns safely in minimum time and discusses the performance of this system when there are errors in position and velocity at the time of abort and in the magnitude and direction of the applied velocity increment. The navigation system presented here uses a simple modification to two-body dynamics to obtain a better approximation to the four-body results.

NOTATION

e	eccentricity
R_e	range from earth
R_m	range from moon
R_s	range from sun
R_p	perigee radius
T	time
V	velocity
V_H	horizontal component of velocity

V_R	radial component of velocity
V_{HO}	initial horizontal component of velocity
V_{RO}	initial radial component of velocity
V_p	velocity at perigee
X, Y, Z	Cartesian coordinates of vehicle's position
X_m, Y_m, Z_m	Cartesian coordinates of moon's position
X_s, Y_s, Z_s	Cartesian coordinates of sun's position
ΔV	incremental velocity
ΔV_p	incremental perigee velocity
γ	flight-path angle
θ	true anomaly
ρ	dimensionless coefficient, R_p/R_e

Superscripts

$(\dot{})$	derivative with respect to time
$(\overline{})$	vector quantity

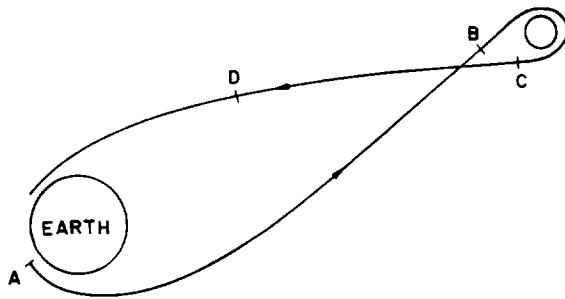
Subscripts

e	earth
H	horizontal
i, j, k	unit vectors on Cartesian axis
m	moon
O	initial value
p	perigee
R	radial

PRELIMINARY CONSIDERATIONS

Applicable Midcourse Regions

As noted in the introduction, aborts considered here are based on a decision to reduce the remaining flight time to the smallest possible value consistent with a safe atmosphere entry but without regard to the touchdown point. This approach leads naturally to separating a circumlunar trajectory into three phases as shown in sketch (a). From the launch at point A to some point B, the location



Sketch (a)

of which is fixed by the available on-board fuel, flight time can be reduced by preventing the circumlunar phase of flight with an abort maneuver. Beyond point B no time can be saved by use of on-board thrust until perilune is passed. From perilune to point C on-board thrust can reduce flight time but calculation of the abort velocity increment is undesirably complex this close to the moon. Beyond point C the abort maneuver is less critical and flight time can be

reduced at the expense of increased entry velocity. Minimum time aborts are not feasible beyond point D since the potential reduction in flight time decreases and the entry velocity penalty increases as the abort point is moved nearer the earth.

This report then, presents data for aborts initiated on the outbound leg of the trajectory from point A to B and on the inbound leg of the trajectory from point C to D.

To examine these abort considerations in a quantitative manner a ballistic circumlunar trajectory starting from Cape Canaveral on February 10, 1966, was selected as a reference. The details of this trajectory are considered later.

After preliminary investigation, point C was fixed somewhat arbitrarily at the moon's nominal sphere of influence boundary (66,000 km) and point D was taken at 200,000 km from the earth. The value for point D was selected after considering the approximate relationship for the increase in perigee velocity associated with inbound aborts with constant perigee.

$$\Delta V_p = \Delta V \left(\frac{V}{V_p} \right)$$

When the distance from the earth is large, the velocity of the spaceship is small and the quantity in the brackets is small, increasing at 200,000 km to 0.134 for the reference trajectory.

Fuel Available

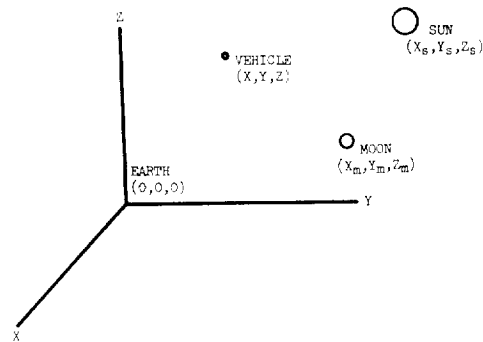
The amount of fuel available for abort purposes on the lunar orbiting mission will be substantial since a velocity increment of roughly 1 km/sec is needed near perilune to put the space vehicle into circular orbit about the moon, and another velocity change of nearly the same magnitude is needed to depart from the moon and return to the earth. With an allowance for midcourse corrections and a reserve there will be a velocity increment of about 2 km/sec available for emergencies while approaching the moon.

For a strictly circumlunar mission there need not be as much fuel on board. Results are presented in this report for velocity increments from 1/2 to 2-1/2 km/sec. Abort performance falls off markedly below the level of 1/2 km/sec.

ANALYSIS

The Mathematical Model

In the development of the equations of motion a restricted four-body system was assumed with a spherical and homogeneous sun and moon. The second harmonic term of the earth's oblateness was included. The coordinate system is Cartesian and geocentric with the Z axis along the earth's polar axis, positive to the north. The positive X axis is in the direction of the vernal equinox and the Y axis is oriented to form the right-handed system shown in sketch (b).



Sketch (b)

The equations of motion are, from reference 4:

$$\ddot{X} = \frac{\mu_e X}{R_e^3} \left[1 + J \left(\frac{a}{R_e} \right)^2 \left(1 - 5 \frac{Z^2}{R_e^2} \right) \right] - \frac{\mu_m}{\Delta_m^3} (X - X_m) - \frac{\mu_m X_m}{R_m^3} - \frac{\mu_s (X - X_s)}{\Delta_s^3} - \frac{\mu_s X_s}{R_s^3}$$

$$\ddot{Y} = \frac{\mu_e Y}{R_e^3} \left[1 + J \left(\frac{a}{R_e} \right)^2 \left(1 - 5 \frac{Z^2}{R_e^2} \right) \right] - \frac{\mu_m}{\Delta_m^3} (Y - Y_m) - \frac{\mu_m Y_m}{R_m^3} - \frac{\mu_s (Y - Y_s)}{\Delta_s^3} - \frac{\mu_s Y_s}{R_s^3}$$

$$\ddot{Z} = \frac{\mu_e Z}{R_e^3} \left[1 + J \left(\frac{a}{R_e} \right)^2 \left(3 - 5 \frac{Z^2}{R_e^2} \right) \right] - \frac{\mu_m}{\Delta_m^3} (Z - Z_m) - \frac{\mu_m Z_m}{R_m^3} - \frac{\mu_s (Z - Z_s)}{\Delta_s^3} - \frac{\mu_s Z_s}{R_s^3}$$

where

$$R_e = \sqrt{X^2 + Y^2 + Z^2}$$

$$R_m = \sqrt{X_m^2 + Y_m^2 + Z_m^2}$$

$$R_s = \sqrt{X_s^2 + Y_s^2 + Z_s^2}$$

$$\Delta_m = \sqrt{(X - X_m)^2 + (Y - Y_m)^2 + (Z - Z_m)^2}$$

$$\Delta_s = \sqrt{(X - X_s)^2 + (Y - Y_s)^2 + (Z - Z_s)^2}$$

$$\mu_e = 3.986135 \times 10^{14} \text{ m}^3/\text{sec}^2$$

$$\mu_m = 4.89820 \times 10^{12} \text{ m}^3/\text{sec}^2$$

$$\mu_s = 1.3253 \times 10^{20} \text{ m}^3/\text{sec}^2$$

$$a = \text{equatorial radius of the earth} = 6.37826 \times 10^6 \text{ m}$$

$$J = 1.6246 \times 10^{-3}$$

The terms involving only distances between the earth and moon or earth and sun, such as $\mu_m X_m / R_m^3$, arise from the fact that the coordinate system is not inertial. These terms account for the acceleration of the coordinate system with respect to inertial space.

The equations of motion for the vehicle are solved by means of a Cowell "second-sum" method. A fourth-order Runge-Kutta method is used to start the integration and to change the step size during the flight. The position of the sun and the moon are determined by interpolation of data from magnetic tape ephemerides. Within the sphere of influence of the moon, taken as 66,000 km from the moon, the origin of coordinates is translated to the center of the moon.

All abort trajectories obtained with this mathematical model resulted from perfect abort maneuvers; that is, the knowledge of position and velocity before abort was exact and there was no error in the control of the magnitude and direction of the abort thrust. Following such a maneuver, a trajectory to perigee was computed with the four body simulation. Error analyses were then made for deviations about these nominal abort trajectories.

The Two-Body Analysis

The objective throughout this report is to determine the thrust direction which will return the space vehicle to earth in minimum time and, naturally, it is desired to make this determination the simplest compatible with satisfactory accuracy. There are design restrictions which must be satisfied because of the limited fuel supply or velocity increment capability, and the necessity of achieving safe entry conditions.

The four-body nonlinear differential equations of motion given previously are difficult to solve and it is unlikely that a simple means for predicting abort velocity requirements will be derived from them. The equations that describe the motion of a space vehicle of negligible mass moving in the gravitational field of a spherical homogeneous earth are much simpler. This restricted two-body system has known solutions in which the quantities of interest are related by algebraic equations rather than differential equations; consequently, a two-body analysis is very advantageous if sufficient accuracy can be attained. Therefore, in the following paragraphs an equation will be developed, based on the two-body system just discussed, which specifies the velocity increment and reentry conditions. Later, suitable corrections will be added for the secondary effects presently neglected.

On lunar trajectories, satisfactory entry conditions may be expressed by a specified vacuum perigee. In this report a specified perigee of 6,450 km is considered. With this perigee and with eccentricities between 0.85 and 1.15, it may be determined from the relation

$$\frac{\dot{R}_e}{R_e \dot{\theta}} = \tan \gamma = \frac{1}{R_p \sqrt{1+e}} \sqrt{-R_p^2(1+e) + 2R_e R_p - R_e^2(1-e)}$$

that the flight-path angle at 400,000 feet (121.92 km) is $-5.0 \pm 0.25^\circ$.

Consider now the two-body system previously mentioned, the space vehicle of negligible mass moving in the gravitational field of a spherical homogeneous earth. In this system the minimum time to return to a prescribed perigee from a given range with a restricted velocity increment is given by an orbit in the original plane of motion; that is, the orbital plane is not changed by the abort firing. A proof of this fact is given in appendix A.

It has now been shown that a planar analysis is sufficient to develop the proposed two-body prediction equation. The development is continued with the general equation of a conic trajectory,

$$v^2 = \frac{2\mu_e}{R_e} - \frac{\mu_e(1-e)}{R_p}$$

and at perigee

$$v_p^2 = \frac{2\mu_e}{R_p} - \frac{\mu_e(1-e)}{R_p}$$

so

$$v^2 - v_p^2 = 2\mu_e \left(\frac{1}{R_e} - \frac{1}{R_p} \right)$$

Since the angular momentum of the vehicle immediately after an abort is the same as the momentum at perigee, we have

$$v_p = \frac{R_e v_H}{R_p}$$

also

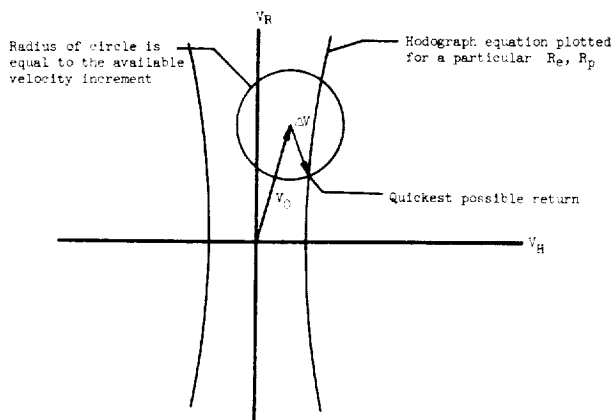
$$v^2 = v_H^2 + v_R^2$$

Substituting these two equations into the previous one gives the hodograph equation

$$v_H^2 = \frac{R_p^2}{R_e^2 - R_p^2} v_R^2 + \frac{2\mu_e R_p}{R_e} \left(\frac{1}{R_e + R_p} \right) \quad (1)$$

This is another form of the general conic equation. Now if R_p is a fixed vacuum perigee height and if R_e is a fixed range at which the abort firing is to be accomplished, then the velocity vector after abort must satisfy this equation; that is, any conic trajectory, of whatever eccentricity, as long as it has the desired perigee height satisfies this equation at any specified range. A quantitative picture of the velocities which must exist after an abort firing is given in figure 1 for $R_p = 6,450$ km and various ranges, R_e .

The total velocity vector achievable by an abort firing is determined by the components of the velocity just before abort, v_{R0} and v_{H0} , and the fuel supply or velocity increment capability available. Graphically, the achievable velocities which will effect a safe entry are those that lie within the circle and also lie on the hodograph plot in sketch (c).



Sketch (c)

Examination of this sketch shows several possibilities. If the circle of achievable velocities is very small, corresponding to a negligible velocity increment, no solutions will exist. Physically, this corresponds to a space vehicle which has run out of fuel or has a badly damaged engine. Without some velocity increment capability the reentry conditions cannot be changed.

If the circle of achievable velocities is somewhat larger, or if the symmetrical branches of the hodograph are closer together because of increased range (see fig. 1), then there will be one branch of the hodograph going through the circle as shown in sketch (c).

The third possibility is that both branches of the hodograph will go through the circle of achievable velocities. The usual situation for the data considered in this report is that the velocity increment and the range are both large; therefore, the circle intersects both branches.

The solution on the left branch of the curve corresponds to an abort maneuver in which the direction of the spacecraft's orbit about the earth is reversed. This will result in retrograde reentries which are undesirable because of the higher velocity of the spacecraft relative to the atmosphere rotating with the earth, but they may be tolerable and they must be considered in point return analyses. These left-branch returns are not considered further in this report since it is shown in appendix B that the minimum flight time to perigee is associated with that achievable hodograph point for which V_R is an algebraic minimum. This point, marked in sketch (c), is always on the right-hand branch of the hodograph. To obtain the components of velocity which give the minimum flight time return a fourth-order algebraic equation must be solved. This prediction equation is derived in appendix C.

Effects of Two-Body Analysis

When the direction of the abort rocket firing is determined with a scheme that ignores the moon and the sun, substantial error is incurred. Figure 2 shows the perigee miss distance as a function of range for aborts from the base trajectory. Near the earth, as expected, two-body predictions suffice, but at only 100,000 km, the 0.50 km/sec velocity increment abort misses desired perigee by 290 kilometers. With larger velocity increments the error is reduced since there is less return time for the moon-sun effects to perturb the intended abort trajectory, and the apogee of the return trajectory is less distant from the earth. The data in figure 2 show that the error is far too great for most cases of interest and this establishes the fact that predictions of abort velocity requirements cannot ignore the effects of both the moon and the sun.

On lunar trajectories with approximately the same enroute times, the lunar perturbations will vary only slightly with the particular day or month of launch since the geometry of the earth-moon-vehicle relationship is essentially constant. The major effect of the moon's gravitational pull might then, with reasonable generality, be incorporated into the prediction equation to materially shrink the lunar bias. To ascertain the validity of this approach, some computer runs were made to isolate the perturbations due to the moon and the sun separately. The gravitational constant of the sun was set equal to zero for one series of runs, and then another series was run with the gravitational constant of the moon set equal to zero. These results are presented in figures 3 and 4.

These figures show that the gravitational pull of the moon has the larger effect but they also show that the gravitational pull of the sun is substantial if either the range at abort is large or only moderate amounts of fuel are available. It is now apparent that even if the lunar bias were reduced to an acceptable level by some general modification of the two-body analysis, the errors in the prediction of perigee would still be too large for many cases of interest because of the sun.

The earth-sun-vehicle geometry is not constant, and it is felt that an effort toward generality here would call for an unwarranted amount of complexity in on-board equipment. Thus, it was concluded that each lunar trajectory should be treated individually.

Modified Two-Body Analysis

With these facts in mind, the two-body prediction equation was adapted for the reference trajectory in a very simple fashion. In shooting a rifle at a target a substantial distance away, one soon learns to use the sights (or prediction system) of the rifle in a modified fashion by aiming above the target to allow for the drop due to gravity. This same simple principle was applied to the two-body equation developed in appendix C.

It is desired to hit a perigee of 6,450 km. When the prediction equation was used with a given velocity increment, range at abort, and a desired perigee of 6,450 km, it was observed that the perigee achieved was equal to 6,450 km minus an error term. Figure 2 illustrates these results.

The modified procedure is to use the prediction equation with the same velocity increment, the same range at abort, and a perigee equal to 6,450 km plus the error term. This is directly analogous to target shooting; if your first shot falls five feet below the target then when you fire the second shot your sights are set on a point five feet above the target.

When the two-body equation was furnished with a velocity increment, a range at abort, and a perigee equal to 6,450 km plus the error term, then the perigee miss distance was reduced. The perigee achieved was equal to 6,450 km minus a second error term, which is much smaller than the first error calculated. If this aiming principle is applied again with a velocity increment, a range at abort, and a perigee equal to 6,450 km plus the first and second error terms, then a further reduction in miss distance will be obtained.

All the modified two-body prediction-equation data presented in this report were obtained by using in the equation a perigee equal to 6,450 km, plus the first and second error terms. This was sufficient to reduce the perigee miss distance to a practical level throughout the entire range of aborts considered.

Table I shows how effectively the moon-sun bias was reduced. The unmodified results are taken from the graph in figure 2 and are tabulated for convenience in comparing the results. Out to 250,000 km the perigee miss distance is negligible. Some error exists at 300,000 and 350,000 km, but it is only appreciable at the lower abort velocity increments, and it is shown later that these range-velocity increment combinations are not likely to be used. It is, of course, also true that the intended trajectory and the actual trajectory achieved by the space vehicle will differ somewhat because of injection errors and abort thrust errors so that it would be pointless to refine this prediction scheme further.

This modification to the two-body equation is based on the vehicle's being on a reference trajectory and it is pertinent to discuss the sensitivity of the

scheme to deviations from this reference trajectory. It was felt that the sensitivity to position deviations would be small since the scheme works on range, and the four-body geometry is not altered appreciably by a few hundred kilometers of horizontal deviation. In an actual trajectory, velocity deviations before abort should be small since the crew has direct control over velocity and will periodically make a correction with vernier rockets. However, a digital simulation was made to obtain some data on this point. A trajectory was computed for launch conditions identical to the base run except that the launch velocity magnitude was increased 0.50 meter/sec. Aborts from this trajectory, using a velocity increment of 1.50 km/sec, had perigee errors of less than 5.0 km even at a range of 300,000 km where a horizontal deviation of 311 km occurred. This was highly satisfactory and consequently no further data were obtained on this point.

Error Analysis

Certain errors will appear in the abort maneuver regardless of the manner in which the abort maneuver is mechanized. The errors considered in this report are the inaccuracy in the knowledge of position and velocity at abort and the imperfect control of the magnitude and direction of the thrust during abort. The statistical effects of these errors upon the perigee distance attained have been computed in this report.

A root-mean-square estimate of the errors in position and velocity was attained following the analysis of Smith in reference 5 wherein optical instrumentation, with Gaussian errors of approximately 10 arc seconds magnitude, was assumed. This analysis employed statistical filter theory to obtain an optimal estimate of position and velocity from the observations available. An observation schedule, detailed in appendix D, involving only 40 observations on the way to the moon was used in the present report.

From the rms estimate of the errors in position and velocity, the techniques presented by McLean in reference 4 were used to predict root-mean-square errors in perigee caused by position and velocity information. This involves a linear prediction scheme about a reference trajectory.

The imperfect control of magnitude and direction of the abort thrust was studied using a matrix analysis illustrated by Battin in reference 6 where the errors in magnitude and direction are independent random variables. The errors were not restricted to the plane of the orbit, and they were assumed to be Gaussian.

RESULTS AND DISCUSSION

Primary Data

A summary of the data obtained relating minimum return time to the range at abort is presented in figures 5(a) and 5(b) for the outbound and return legs of the circumlunar trajectory. The minimum time to return naturally diminishes with

increasing amounts of abort velocity capability, but it is observed that the increase in performance obtained in going from 0.50 km/sec to 1.0 km/sec is very marked. At less than 0.50 km/sec the abort capability is marginal. Indeed, figure 6, a plot of total time from injection to perigee versus range at abort, shows that an abort which is accomplished at outbound ranges greater than 277,000 km with 0.50 km/sec, is valueless since a quicker return is accomplished by doing nothing. It is interesting to note that for the lower abort velocities, it is possible to return more quickly by aborting on the return leg of the mission even before the space vehicle has accomplished half of the trip, in terms of hours, to the moon. The data of figure 6 determine the location of point B in sketch (a).

The error analysis techniques previously discussed were applied to abort trajectories calculated with the modified two-body equation. The calculations to obtain the root-mean-square errors in the knowledge of position and velocity resulted in position errors of the order of 50.0 kilometers and velocity errors around 5.0 m/sec. The maximum rms effect of these errors at perigee, due to both position and velocity errors simultaneously, was 17.0 kilometers. These results for the outbound leg are shown in table II. The rms errors obtained are dependent on the observation schedule and more particularly on the relation of the time of abort to the observation schedule, the errors being smaller after an observation when the position and velocity are known most accurately. The data shown here were obtained from abort just prior to an observation when the position and velocity are known least accurately. These errors are tolerable and it follows then that abort considerations do not necessitate an increased number of celestial observations for better determination of position and velocity. These data also substantiate the argument that the modified two-body equation is not sensitive to deviations from the reference trajectory.

A statistical estimate of the deviation in perigee height due to faulty control of the magnitude of the abort rocket thrust was obtained. A 1-percent root-mean-square deviation in the thrust magnitude produced the surprisingly small errors observed in figure 7. A 1-percent error in a 2-1/2 km/sec abort is a velocity error of 25 m/sec, which is very large relative to normal burnout errors. These data show that perigee height is very insensitive to errors in velocity magnitude along the thrust axis of the minimum time abort. This thrust axis is primarily along the radius vector from the earth to the vehicle.

This marked insensitivity becomes understandable if the general conic equation, in the previously developed hodograph format, is reexamined and the partial derivatives $\partial R_p / \partial V_R$ and $\partial R_p / \partial V_H$ are evaluated from it. These partial derivatives are:

$$\frac{\partial R_p}{\partial V_R} = - \frac{R_p^2}{\mu_e e} (V_R)$$

$$\frac{\partial R_p}{\partial V_H} = \frac{R_e^2 - R_p^2}{\mu_e e} (V_H)$$

and

$$\frac{\partial R_p}{\partial V_R} \div \frac{\partial R_p}{\partial V_H} = - \frac{R_p^2}{R_e^2 - R_p^2} \frac{V_R}{V_H}$$

Now if R_e is greater than 100,000 km, about 16 R_p , then

$$\frac{\partial R_p}{\partial V_R} \div \frac{\partial R_p}{\partial V_H} < \left| \frac{1}{255} \frac{V_R}{V_H} \right| < \frac{1}{127.5}$$

since V_R is less than 2.0 V_H at these distances. Thus, for the ranges considered, a unit error in radial velocity after abort is less than one-hundredth as significant as a unit error in horizontal velocity after abort. This implies that when velocity correction mechanisms are designed for the lunar mission, particular attention should be given to the horizontal component errors.

Since the minimum time return requires the abort thrust to be fired almost radially, errors in the aiming of the abort rocket will produce, almost exclusively, velocity errors in the horizontal plane. By the analysis of the previous paragraph these errors should be significant. Indeed, perigee errors resulting from aiming inaccuracies of the abort rocket are of major significance and appear to be the only serious errors when the modified two-body equation is used. These aiming error data are shown on figures 8(a) and 8(b) for the outbound and inbound legs of the trajectory, respectively. An rms error of 0.50° in aiming the abort velocity vector was assumed. The perigee error from this source ranges from 50 to 300 km for an abort at only 100,000 km, on the outbound leg with velocity increments of 0.50 to 2.50 km/sec.

Midcourse Correction Following an Abort

Since it is likely that substantial error will be incurred in the abort maneuver, it is necessary to judge how much fuel should be saved for a vernier firing near the earth. Sufficient information is contained in the hodograph equation to make this judgment when prospective perigee errors are known. The velocity increment required to correct a perigee error does not change very much with the source of the error as is shown in figure 9. The central curve on this figure is an expanded scale version of the $R = 100,000$ kilometer curve in figure 1. It should be noted that the abscissa scale is expanded a hundred times more than the ordinate. Also shown on the curve is hodograph data for values of $R_p \pm 300$ kilometers away from the nominal value. Examination of this graph shows that the velocity increment required to correct from any trajectory with perigee of 6,750 km to a trajectory with perigee of 6,450 km is never as much as 20 m/sec if the correction is applied at 100,000 km. The applicable area of the hodograph plot is further restricted by the knowledge that aborts on the way to the moon have eccentricities less than 1 while aborts after perilune have eccentricities between 0.98 and 1.13.

The penalty caused by making the velocity correction at 20,000 km rather than at 100,000 km can be ascertained with the aid of figure 10 which presents hodograph data for a range of 20,000 km and for all trajectories having perigee errors of ± 300 km and 0. Here it is shown that the velocity increment required to correct from any trajectory with perigee of 6,750 km to a trajectory with perigee of 6,450 is never more than 110 m/sec if the correction is applied at 20,000 km. In this example then, delaying the correction until the space vehicle is quite near the earth (20,000 km) costs an extra 80-90 m/sec of velocity increment. It should be noted that because of the different ordinate and abscissa scales used in figure 10, the minimum velocity increment between the two curves is not the perpendicular distance between the curves but more nearly the horizontal distance between these curves.

Over-all, it is interesting to note that the large end-point error of 300 km requires a velocity increment correction which is only a few percent of the abort velocity increment, if the correction is made at 100,000 km.

Graphical Prediction of an Abort Maneuver

An extremely simple abort scheme is possible with hodograph data displayed in figures 9 and 10. If the astronaut can reasonably estimate range, radial velocity, and horizontal velocity, he can accomplish a safe return even though both the on-board computer and communications from earth have failed. Preprinted graphical representations of the hodograph equation at many ranges together with current estimates of range and the velocity components give sufficient information to determine a satisfactory direction and magnitude of the rocket thrust. The astronaut can choose either the least velocity increment necessary to give the space vehicle velocity components which lie on the hodograph for the desired perigee, saving substantial fuel for further corrections, or any larger velocity increment available to him which will decrease the return time.

Figures 1, 9, and 10 are drawn directly from the general conic equation in the hodograph format. That is, they present two-body equation information for returning to a desired vacuum perigee. Similar curves can be drawn from the results of modified two-body equation calculations. Thus the effects of the moon and the sun on the reference trajectory can be incorporated into the velocity component presentation given the astronaut.

CONCLUSIONS

A modified Keplerian orbit was used in a midcourse abort study for determining the direction of the abort thrust that will achieve a minimum time return. The minimum time return calculation provides the information needed for evaluating the time penalty associated with a fixed point abort. Aborts were considered on both the outbound and return legs of the flight.

The errors in making the abort maneuver and their effects on the abort trajectory were investigated. The velocity increments necessary to correct the errors introduced at abort were computed at various ranges on the return leg of the abort.

From the results of this study the following conclusions can be drawn:

1. The modified two-body equation developed in this study is sufficiently accurate for determining the direction of the abort thrust to achieve a minimum time return to satisfactory entry conditions.

2. The modified two-body equation is based on the vehicle's being on a reference trajectory but the vacuum perigee is predicted with satisfactory accuracy when the vehicle is substantially off the reference trajectory.

3. Perigee altitude was found to be insensitive to errors in knowledge of position and velocity before abort; and also to errors in the magnitude of the abort velocity increment. However, small errors in aiming the abort rocket resulted in very large perigee altitude errors. Even though the abort maneuver may introduce large perigee errors, a vernier correction made at a range of 100,000 kilometers from the earth would require less than 5 percent of the abort velocity increment to null the root-mean-square perigee error.

4. Abort performance falls off markedly below a velocity increment capability of 0.50 km/sec. For these lower velocity capabilities, there is only a limited region on the outbound leg where an outbound abort has a time advantage over an inbound abort.

5. If a reasonable estimate of range, radial velocity, and horizontal velocity can be made, a safe return can be accomplished even though both the on-board computer and the communications from the earth have failed. Preprinted graphical representations of the hodograph equation at various ranges, together with current estimates of these quantities, give sufficient information to determine the direction and magnitude of the rocket thrust required.

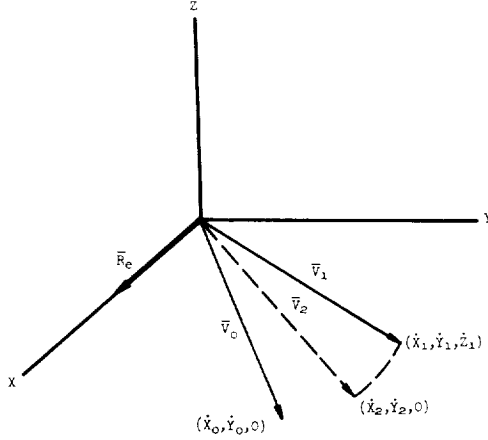
Ames Research Center
National Aeronautics and Space Administration
Moffett Field, Calif., Jan. 3, 1963

APPENDIX A

CONSTANCY OF ORBIT PLANE

It is the purpose of this appendix to show that the minimum time to return to a prescribed perigee from a given range with a velocity increment restriction is given by an orbit in the original plane.

This will be accomplished by demonstrating that if one desires to change from a given orbit to another orbit, with specified conic characteristics but unspecified plane, using a minimum velocity increment, the planes of the two orbits must be the same. This is sufficient to attain the objective of this appendix because it may then be argued that if e_1 and T_{p1} are the best out of plane conic characteristics available, these same conic characteristics can be obtained in plane with a lesser velocity increment. The difference in velocity increments can then be used to further reduce T_{p1} .



Sketch (d)

Let the vehicle be anywhere on its orbit. Choose an earth-centered axis system with the positive X axis through the vehicle and the X-Y plane as the original orbit plane, sketch (d).

Let $\bar{V}_1 = \dot{X}_1\bar{i} + \dot{Y}_1\bar{j} + \dot{Z}_1\bar{k}$ be the velocity vector which together with the initial \bar{R}_e determines a trajectory with the desired conic characteristics. If we rotate the \bar{R}_e, \bar{V}_1 plane about the X axis into the X-Y plane, the velocity vector is now $\bar{V}_2 = \dot{X}_2\bar{i} + \dot{Y}_2\bar{j} + (0)\bar{k}$.

If ϕ is the angle of rotation about the X axis, then

$$\begin{bmatrix} \dot{X}_1 \\ \dot{Y}_1 \\ \dot{Z}_1 \end{bmatrix} = \begin{bmatrix} 1 & 0 & 0 \\ 0 & \cos \phi & \sin \phi \\ 0 & -\sin \phi & \cos \phi \end{bmatrix} \begin{bmatrix} \dot{X}_2 \\ \dot{Y}_2 \\ \dot{Z}_2 \end{bmatrix} \quad \text{or} \quad \begin{aligned} \dot{X}_1 &= \dot{X}_2 \\ \dot{Y}_1 &= \dot{Y}_2 \cos \phi \\ \dot{Z}_1 &= -\dot{Y}_2 \sin \phi \end{aligned}$$

For any value of ϕ , ($0 \leq \phi < 2\pi$) a velocity vector is specified and a plane is determined through \bar{R}_e and \bar{V} . In this plane a trajectory exists, determined by \bar{R}_e and \bar{V} , which has the specified conic parameters.

The velocity increment $\Delta\bar{V} = \bar{V}_1 - \bar{V}_0$ and

$$|\Delta V|^2 = (\dot{X}_1 - \dot{X}_0)^2 + (\dot{Y}_1 - \dot{Y}_0)^2 + \dot{Z}_1^2 = (\dot{X}_2 - \dot{X}_0)^2 + (\dot{Y}_2 \cos \phi - \dot{Y}_0)^2 + \dot{Y}_2^2 \sin^2 \phi$$

$$|\Delta V|^2 = \dot{X}_2^2 + \dot{Y}_2^2 + \dot{X}_0^2 + \dot{Y}_0^2 - 2\dot{X}_0\dot{X}_2 - 2\dot{Y}_0\dot{Y}_2 \cos \varphi$$

and $|\Delta V|^2$ has extremal values at $2\dot{Y}_0\dot{Y}_2 \sin \varphi = 0$ or at $\varphi = 0, \pi$.

Now $\bar{V}_1 = \dot{X}_1\bar{i} + \dot{Y}_1\bar{j} + \dot{Z}_1\bar{k} = \dot{X}_2\bar{i} + \dot{Y}_2 \cos \varphi \bar{j} - \dot{Y}_2 \sin \varphi \bar{k}$ and V_1 is in the X-Y plane for both $\varphi = 0$ and $\varphi = \pi$. If \dot{Y}_0 and \dot{Y}_2 have opposite signs, the minimum value of $|\Delta V|$ is obtained at $\varphi = \pi$ and the maximum occurs at $\varphi = 0$. If \dot{Y}_0 and \dot{Y}_2 have the same sign, the minimum value of $|\Delta V|$ is obtained at $\varphi = 0$ and the maximum value occurs at $\varphi = \pi$. Thus for minimum velocity increment the two orbits are coplanar.

APPENDIX B

MINIMUM TIME TO RETURN REQUIRES MINIMUM V_R

It is the purpose of this appendix to show that the minimum time to return to a prescribed perigee from a given range is associated with the algebraic minimum of available radial velocity components. Equation (B1) below is the previously developed hodograph equation.

$$V_H^2 = \frac{R_p^2}{R_e^2 - R_p^2} V_R^2 + \frac{2\mu_e R_p}{R_e} \left(\frac{1}{R_e + R_p} \right) \quad (B1)$$

Multiplying equation (B1) by $R_e^2 - R_p^2$ and transposing gives:

$$R_e^2 V_R^2 = (R_e^2 - R_p^2)(V_H^2 + V_R^2) - \frac{2\mu_e R_p}{R_e} (R_e - R_p)$$

or

$$V_R^2 = \frac{R_e^2 - R_p^2}{R_e^2} V^2 - \frac{2\mu_e R_p}{R_e^3} (R_e - R_p) \quad (B2)$$

The standard form of the general conic equation is:

$$v^2 = \frac{2\mu_e}{R_e} - \frac{\mu_e}{R_p} (1 - e) \quad (B3)$$

Now by equation (B2) it is clear that if $|V_{R2}| > |V_{R1}|$ then $|V_2| > |V_1|$ for any given R_e and R_p , with $R_e > R_p$. Similarly, by equation (B3) if $|V_2| > |V_1|$ then $e_2 > e_1$; therefore, if $|V_{R2}| > |V_{R1}|$ then $e_2 > e_1$.

It is now sufficient to show that on the outgoing leg, where $V_R > 0$, minimum time and minimum e go together while on the incoming leg, where $V_R < 0$, minimum time and maximum e go together.

The conic equation, in polar coordinates, is:

$$R_e = \frac{\frac{H^2}{\mu_e}}{1 + e \cos \theta}$$

Differentiating this expression and using $R^2 \dot{\theta} = H$ gives

$$\dot{R}_e = \frac{\mu_e e}{H} \sin \theta = \frac{\mu_e e}{H} \sqrt{1 - \cos^2 \theta} = \frac{\mu_e e}{\sqrt{\mu_e R_p} (1 + e)} \sqrt{1 - \cos^2 \theta}$$

$$\dot{R}_e = \frac{dR_e}{dt} = \frac{\sqrt{\mu_e}}{\sqrt{R_p}} \sqrt{\frac{R_e^2 (e - 1) + 2R_e R_p - R_p^2 (e + 1)}{R_e^2}}$$

and

$$dt = \frac{\sqrt{R_p}}{\sqrt{\mu_e}} \frac{R_e}{\sqrt{R_e^2(e-1) + 2R_e R_p - R_p^2(e+1)}} dR_e$$

The time to return to perigee on inbound orbit

$$T_{in} = \int_{R_0}^{R_p} \frac{\sqrt{R_p}}{\sqrt{\mu_e}} \frac{R_e dR_e}{\sqrt{R_e^2(e-1) + 2R_e R_p - R_p^2(e+1)}}$$

where μ_e , R_p , and e are parameters in the integral.

$$\begin{aligned} \frac{dT_{in}}{de} &= \int_{R_0}^{R_p} \frac{R_e \sqrt{R_p}}{\sqrt{\mu_e}} \left(-\frac{1}{2} \right) \frac{(R_e^2 - R_p^2) dR_e}{\left[R_e^2(e-1) + 2R_e R_p - R_p^2(e+1) \right]^{3/2}} \\ &= -\frac{1}{2} \int_{R_0}^{R_p} \frac{1}{\frac{\sqrt{\mu_e}}{R_e \sqrt{R_p}}} \frac{\frac{\mu_e}{R_e^2 R_p}}{\frac{\mu_e}{R_e^2 R_p}} \frac{(R_e^2 - R_p^2) dR_e}{\left[R_e^2(e-1) + 2R_e R_p - R_p^2(e+1) \right]^{3/2}} \end{aligned}$$

$$\frac{dT_{in}}{de} = -\frac{1}{2} \int_{R_0}^{R_p} \frac{\mu_e}{R_e^2 R_p} \frac{R_e^2 - R_p^2}{R_e^3} dR_e \quad (B4)$$

In this form we see how to choose the sign of the radical which determines the sign of the integrand. We may also write:

$$R_e^2(e-1) + 2R_e R_p - R_p^2(e+1) = (R_e - R_p)[(R_e + R_p)e - (R_e - R_p)]$$

so that

$$\frac{dT_{in}}{de} = -\frac{1}{2} \int_{R_0}^{R_p} \frac{R_e \sqrt{R_p}}{\sqrt{\mu_e}} \frac{(R_e + R_p) dR_e}{(R_e - R_p)^{1/2} [(R_e + R_p)e - (R_e - R_p)]^{3/2}} \quad (B5)$$

This integrand has singularities at perigee and at apogee. The apogee singularity does not lie within the region of integration but the perigee singularity is at one end point of the region of integration. However, reference 7 shows that this integral is convergent; therefore, $dT_{in}/de < 0$ for all e . Since T_{in} is a continuous function of e , we now know that T_{in} decreases with every increase in e . Therefore, on the incoming leg the minimum time solution for a given range and perigee altitude is associated with the maximum available eccentricity.

On the outgoing leg orbits with eccentricities equal to or greater than one do not return or have infinite return time. It is only necessary then to consider elliptical orbits so we may write for the time to return to perigee on the outgoing leg:

$$T_{out} = (2\pi) \left[\frac{R_p^3}{\mu_e (1 - e)^3} \right]^{1/2} - T_{in}$$

where the period of the complete elliptical orbit is

$$(2\pi) \left[\frac{R_p^3}{\mu_e (1 - e)^3} \right]^{1/2}$$

$$\frac{dT_{out}}{de} = (2\pi) \left[\frac{R_p^3}{\mu_e} \right]^{1/2} \left(-\frac{3}{2} \right) (1 - e)^{-5/2} (-1) - \frac{dT_{in}}{de}$$

Both terms here are positive for all $e < 1.0$. Therefore, on the outgoing leg, the minimum time solution for a given range and perigee altitude is associated with the minimum available eccentricity. Thus it has been shown that the minimum time to return is associated with the algebraic minimum of available radial velocity components.

APPENDIX C

DERIVATION OF THE ABORT-VELOCITY PREDICTION EQUATION

The derivation of the equation, whose solution yields the direction of the abort thrust for a minimum return time trajectory, is obtained by combining the hodograph equation with the equation for the change in velocity.

The hodograph equation is

$$V_H^2 = \frac{\rho^2}{1 - \rho^2} V_R^2 + \frac{2\mu_e \rho}{R(1 + \rho)} \quad (C1)$$

and the equation for the change in velocity, ΔV , is given by

$$(\Delta V)^2 = (V_H - V_{H0})^2 + (V_R - V_{R0})^2 \quad (C2)$$

Solving equation (C1) for V_H , substituting into equation (C2), and clearing yields

$$\left[\frac{1}{1 - \rho^2} V_R^2 - 2V_{R0}V_R + V_{H0}^2 + V_{R0}^2 - (\Delta V)^2 + \frac{2\mu_e \rho}{R(1 + \rho)} \right] \frac{1}{4V_{H0}^2} = \frac{\rho^2}{1 - \rho^2} V_R^2 + \frac{2\mu_e \rho}{R(1 + \rho)} \quad (C3)$$

Letting

$$Q = V_{H0}^2 + V_{R0}^2 - (\Delta V)^2 + \frac{2\mu_e \rho}{R(1 + \rho)}$$

equation (C3) becomes

$$\begin{aligned} \left(\frac{1}{1 - \rho^2} \right)^2 V_R^4 + \left(\frac{-4V_{R0}}{1 - \rho^2} \right) V_R^3 + \left(\frac{2Q}{1 - \rho^2} + 4V_{R0}^2 - \frac{4V_{H0}^2 \rho^2}{1 - \rho^2} \right) V_R^2 \\ + \left(-4QV_{R0} \right) V_R + \left[Q^2 - \frac{8\rho V_{H0}^2 \mu_e}{R(1 + \rho)} \right] = 0 \end{aligned} \quad (C4)$$

Dividing both sides of equation (C4) by $\left(\frac{1}{1 - \rho^2}\right)^2$ gives

$$V_R^4 + \left[-4V_{R0}(1 - \rho^2)\right] V_R^3 + (1 - \rho^2) \left[2Q - 4V_{H0}^2 \rho^2 + 4V_{R0}^2 (1 - \rho^2)\right] V_R^2 \\ + (1 - \rho^2)^2 \left(-4QV_{R0}\right) V_R + (1 - \rho^2)^2 \left[Q^2 - \frac{8\rho V_{H0}^2 \mu_e}{R(1 + \rho)}\right] = 0 \quad (C5)$$

This equation, a quartic, can then be solved for the required value of V_R which may be substituted into equation (C1) to give the required V_H . Such a mathematical solution is fairly lengthy. A graphical solution, however, is quite simple and in many cases is sufficiently accurate.

APPENDIX D

OBSERVATION AND VELOCITY CORRECTION SCHEDULE USED ON OUTGOING TRAJECTORY

Right ascension, declination, and subtended angle of the appropriate body are measured simultaneously at each observation.

T = 0.0 is injection time.

T = 3.5 hr begin 8 earth observations space 0.5 hour apart.

T = 8.0 hr begin 7 moon observations space 0.5 hour apart.

T = 12.0 hr make velocity correction.

T = 24.0 hr begin 4 earth observations space 1.0 hour apart.

T = 28.0 hr begin 8 moon observations space 1.0 hour apart.

T = 36.0 hr make velocity correction.

T = 64.0 hr begin 4 moon observations space 1.0 hour apart.

T = 68.0 hr begin 4 earth observations space 1.0 hour apart.

T = 72.0 hr make velocity correction.

The instruments used in the observations are assumed to have a minimum rms error of 10 arc seconds with a mean of zero. The error increases as observed body is approached.

Abort Rocket: The aiming error here was taken as 0.5° rms with zero mean. In conjunction with the aiming error, calculations were made for a thrust magnitude error of 1.0 percent and also for a flat 1.0 m/sec cutoff error.

Base Trajectory: Injection occurs on Feb. 10, 1966, with $R_0 = 6,499.02$ km, $V_0 = 11.001372$ km/sec, and $\gamma_0 = -1.26 \times 10^{-8}$ deg. Perilune is reached in 83.72 hours and is 5,713 km (1,738 + 3,975).

REFERENCES

1. Kelley, Thomas J., and Adornato, Rudolph J.: Determination of Abort Way-Stations on a Nominal Circumlunar Trajectory. ARS Jour., vol. 32, no. 6, June 1962, pp. 887-93.
2. Miller, James S., and Deyst, John J., Jr.: Preliminary Study of Aborts from Circumlunar Trajectories. Instrumentation Laboratory, MIT Rep. E-1124, March 1962.
3. Slye, Robert E.: Velocity Requirements for Abort From the Boost Trajectory of a Manned Lunar Mission. NASA TN D-1038, 1961.
4. McLean, John D., Schmidt, Stanley F., and McGee, Leonard A.: Optimal Filtering and Linear Prediction Applied to a Midcourse Navigation System for the Circumlunar Mission. NASA TN D-1208, 1962.
5. Smith, Gerald L., Schmidt, Stanley F., and McGee, Leonard A.: Application of Statistical Filter Theory to the Optimal Estimation of Position and Velocity on Board a Circumlunar Vehicle. NASA TR R-135, 1962.
6. Battin, Richard H.: A Statistical Optimizing Navigation Procedure for Space Flight. Instrumentation Laboratory, MIT Rep. R-341, Sept. 1961.
7. Woods, Frederick S.: Advanced Calculus. Boston, Ginn and Company, 1934.

TABLE I.- PERIGEE MISS DISTANCE DATA FOR MODIFIED GUIDANCE LAW

Range at abort kilometers	Miss distance, in kilometers, below $R_p = 6,450$ km for abort velocity of--					
	0.5 km/sec	1.0 km/sec	1.5 km/sec	2.0 km/sec	2.5 km/sec	
50,000 Unmodified Modified	92.3 .1	16.4 0	8.0 0	5.2 0	4.4 0	
100,000	283.7 .8	57.1 0	24.3 0	14.4 0	10.2 0	
150,000	569.9 5.0	139.5 0	62.9 0	37.6 0	2.6 0	
200,000	900.9 22.3	286.5 .3	139.6 0	86.4 0	60.8 0	
250,000	1034.7 55.9	528.1 1.8	280.7 .2	180.9 0	129.8 0	
300,000	--- ---	950.6 11.6	573.7 1.7	388.8 .5	286.8 .2	
350,000	--- ---	--- ---	1257.3 19.9	927.8 5.6	705.4 2.4	

TABLE II.- ROOT-MEAN-SQUARE PERIGEE ERRORS DUE TO ERRORS IN THE
KNOWLEDGE OF POSITION AND VELOCITY AT ABORT

Time from injection, hr	Range, km	Rms perigee errors, km		
		V = 0.5 km/sec	V = 1.5 km/sec	V = 2.5 km/sec
3.5	58,074	17.299	9.806	2.765
8.0	102,397	2.268	1.519	0.903
12.0	133,671	3.036	1.991	1.035
24.0	206,372	7.145	4.483	1.768
60.0	343,954	4.877	3.383	1.846

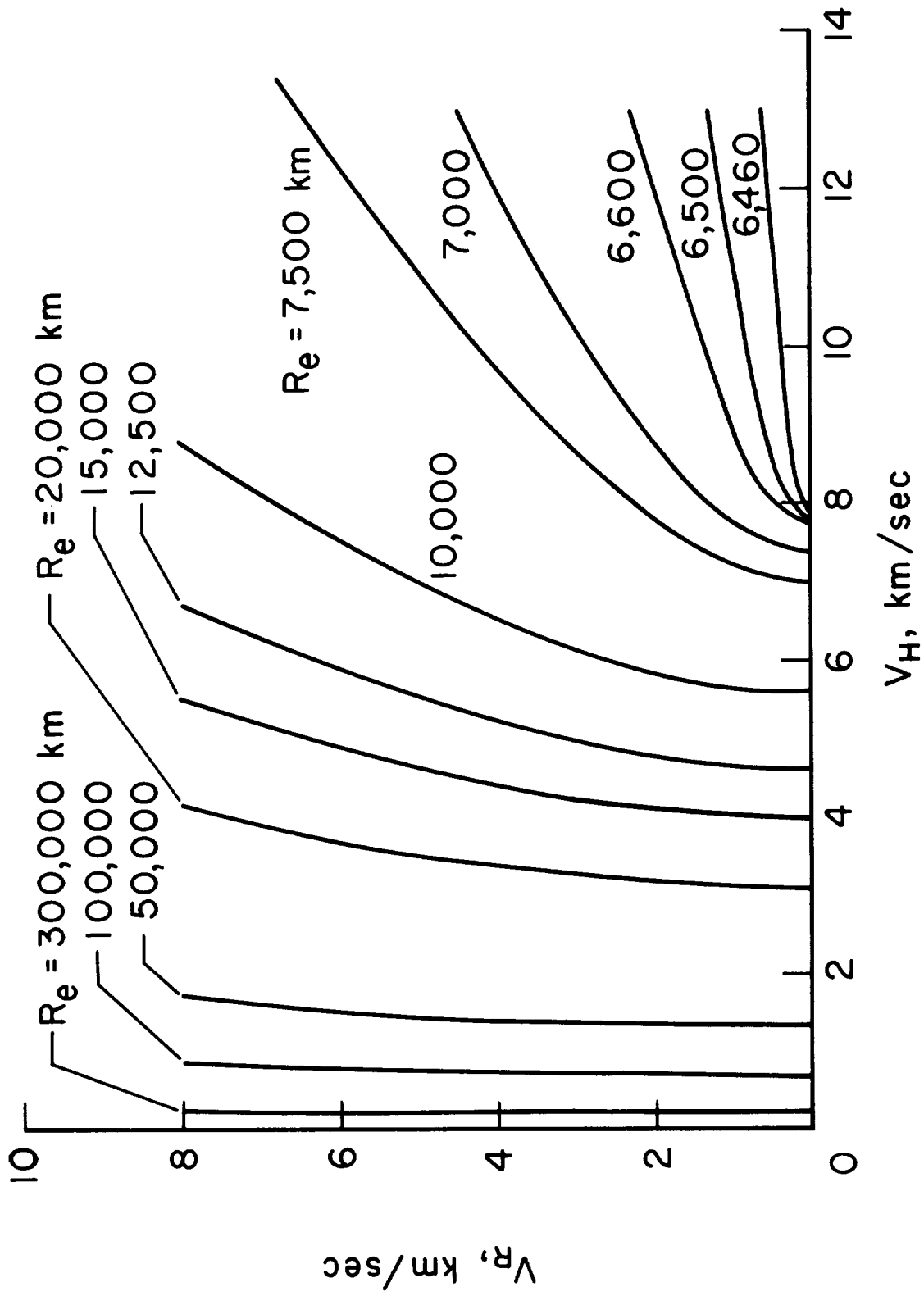


Figure 1.- Velocity hodograph for perigee radius of 6,450 km.

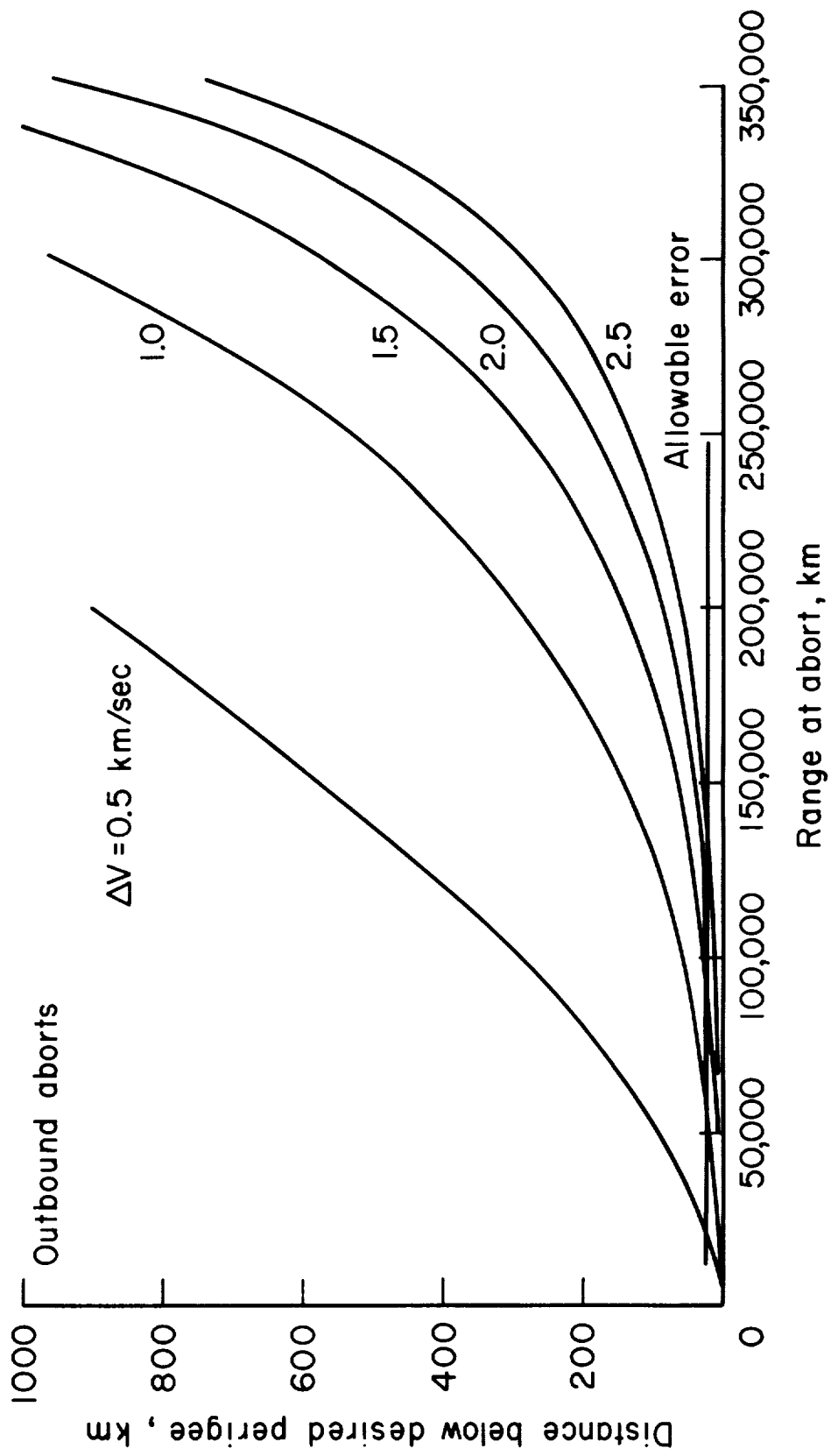


Figure 2.- Perigee miss distance due to two-body guidance law.

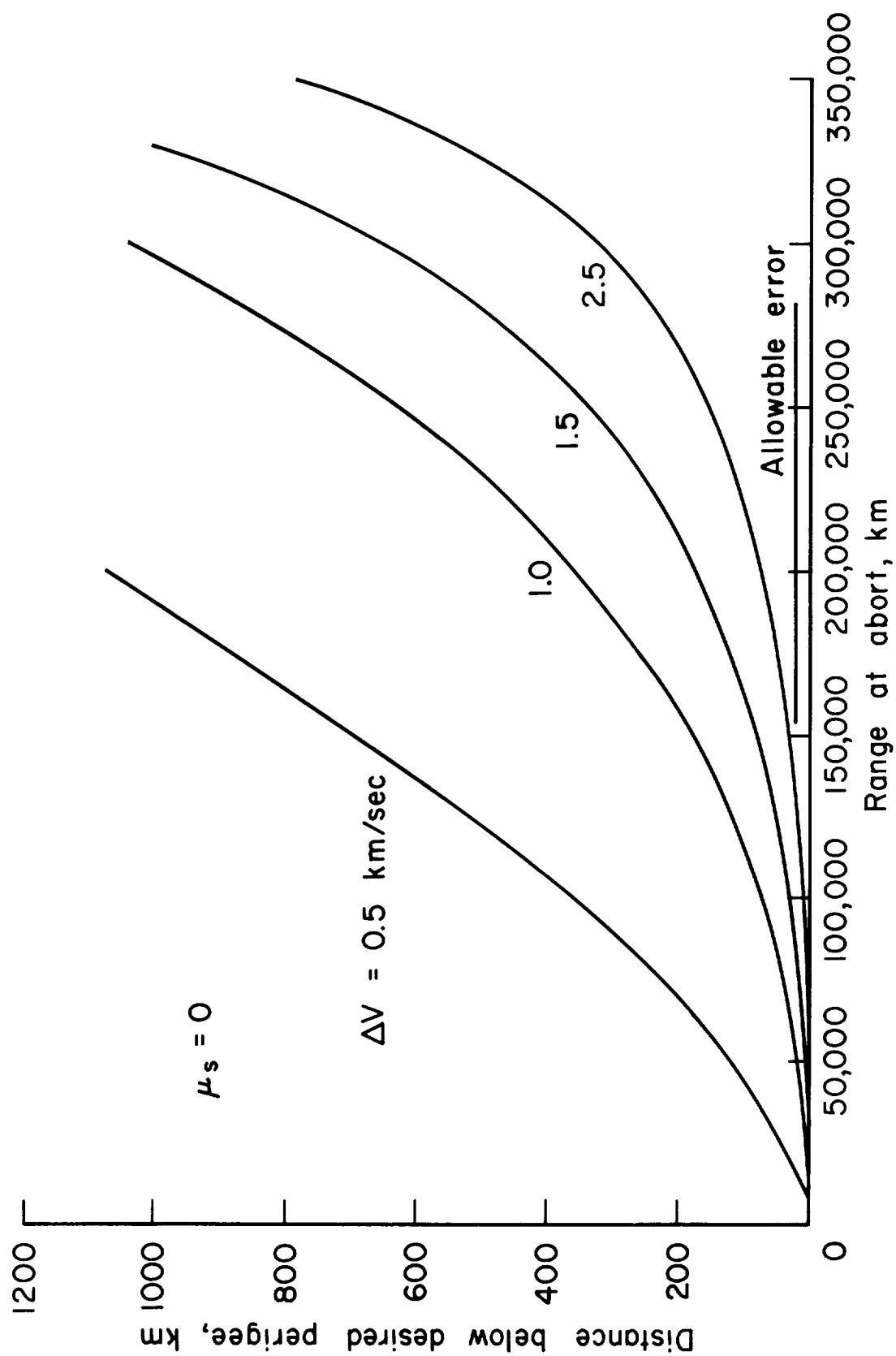


Figure 3.- Perigee miss distance due to moon's effect.

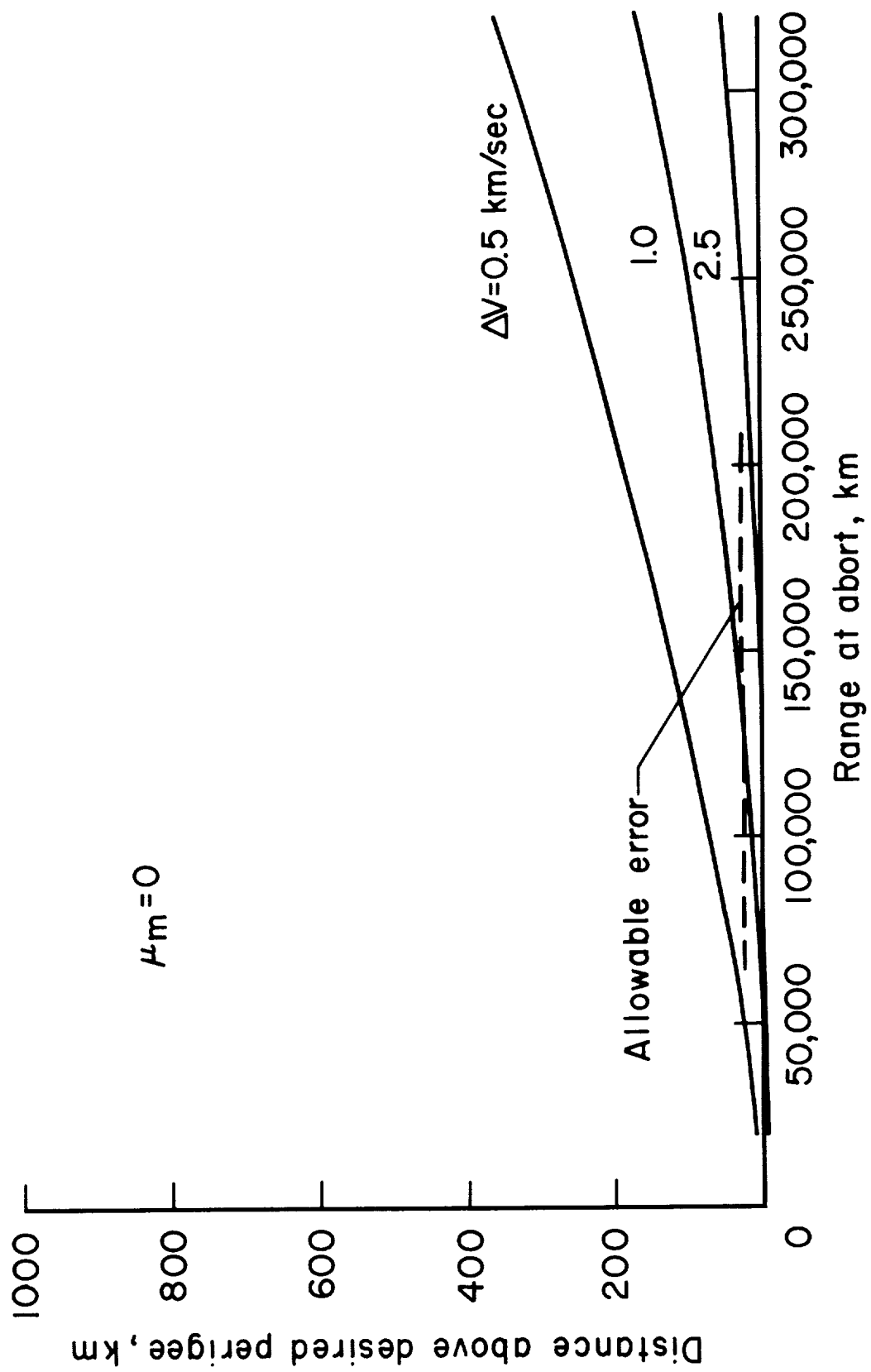


Figure 4.- Perigee miss distance due to sun's effect.

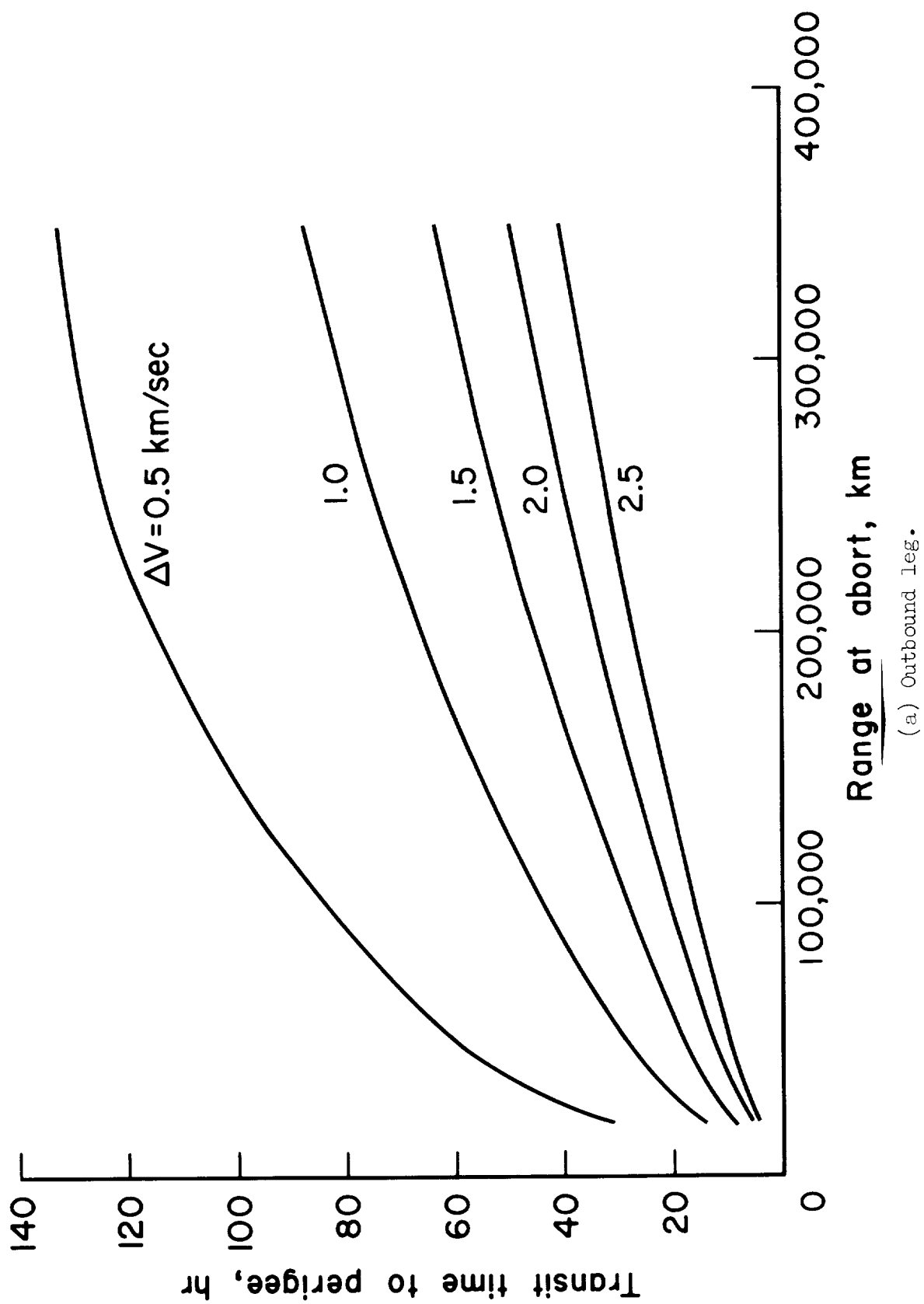
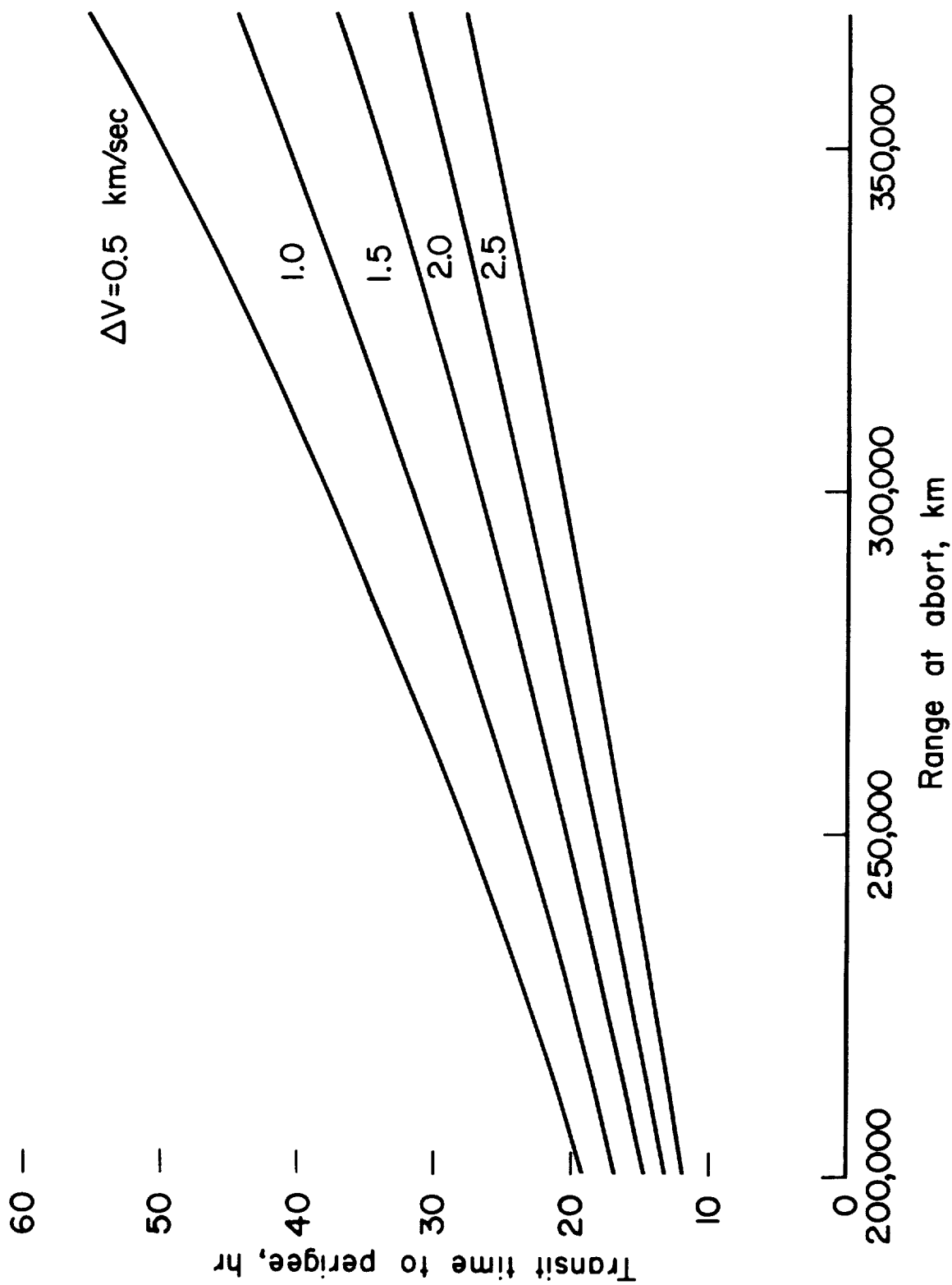


Figure 5.- Flight time from abort to perigee.



(b) Return leg.

Figure 5.- Concluded.

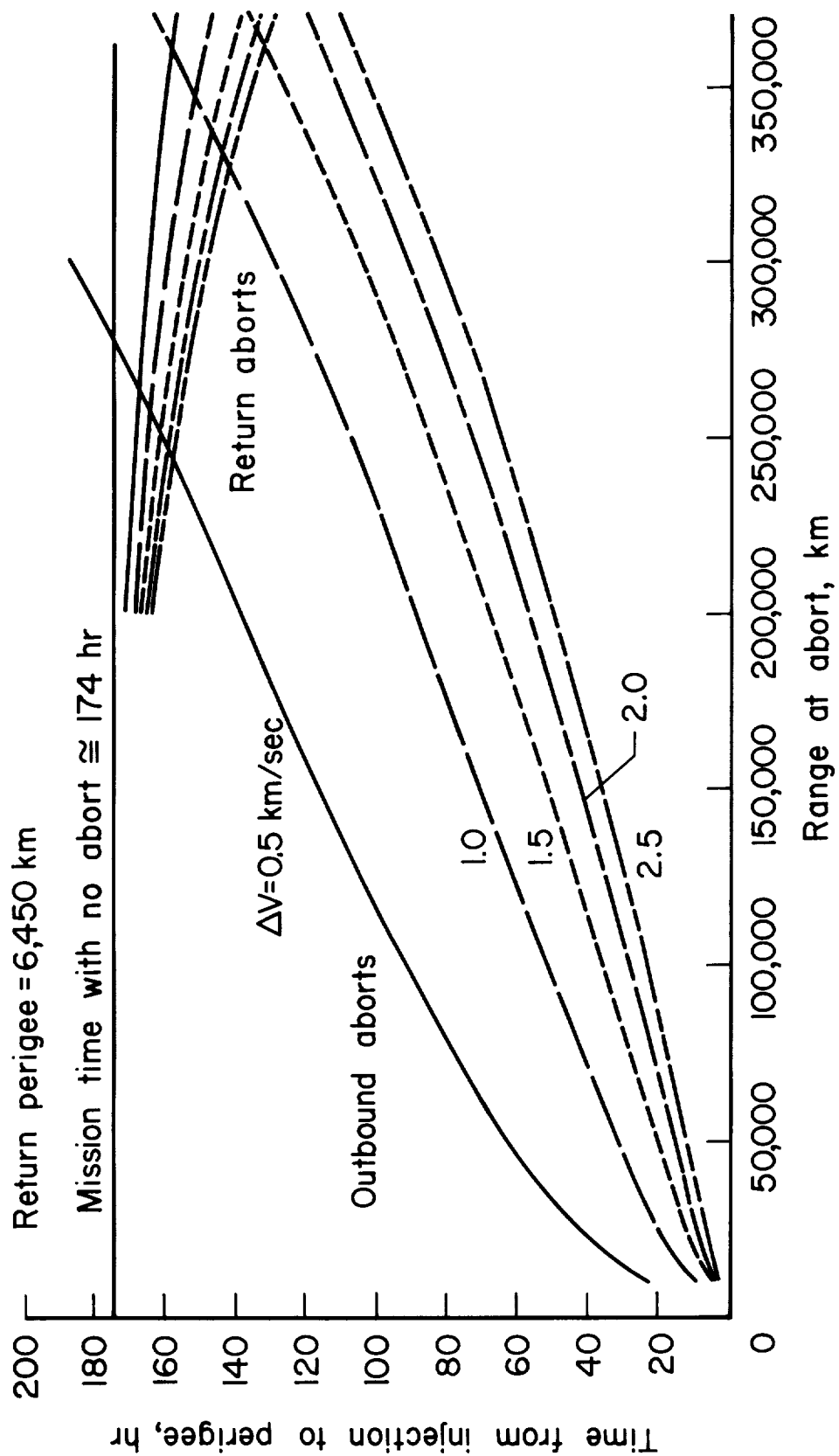


Figure 6.- Total flight time, injection to perigee.

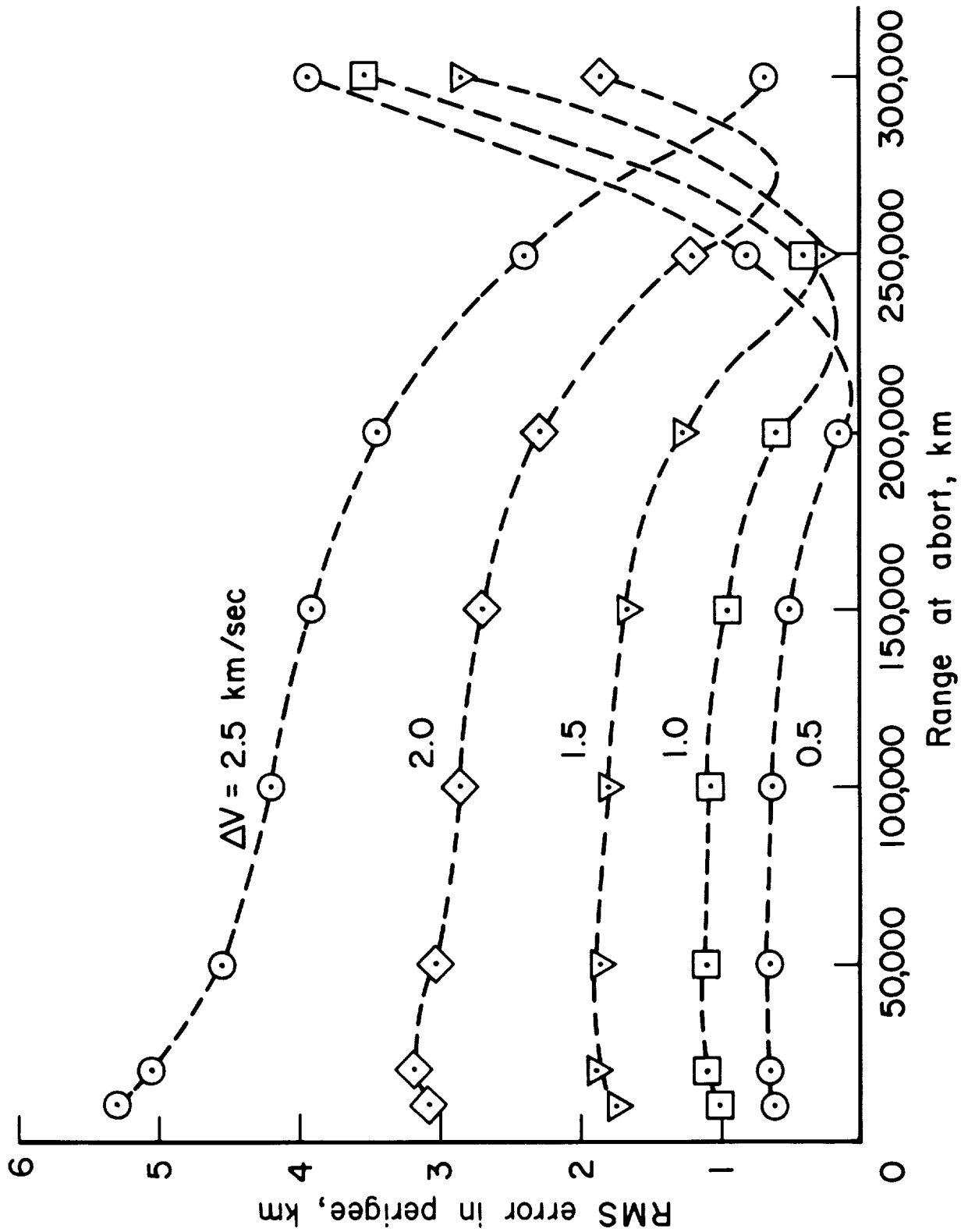


Figure 7.- Root mean square error in perigee due to a 1-percent rms error in thrust magnitude.

0 29 11
SEC CAT ISS
N63-15052
ACCESSION NO.

SECURITY
CLASSIFICATION

CORP AUTHOR
C-5 CODE
1 602110
1
1

MICROFORM
1
YES
NO
OTS

SUPPORTED BY
NASA
NONNASA
1

TRACINGS
6

C-9 PERSONAL AUTHORS
1 Merrick, R. B.
1 Callas, G. P.
1
1

N63-15052

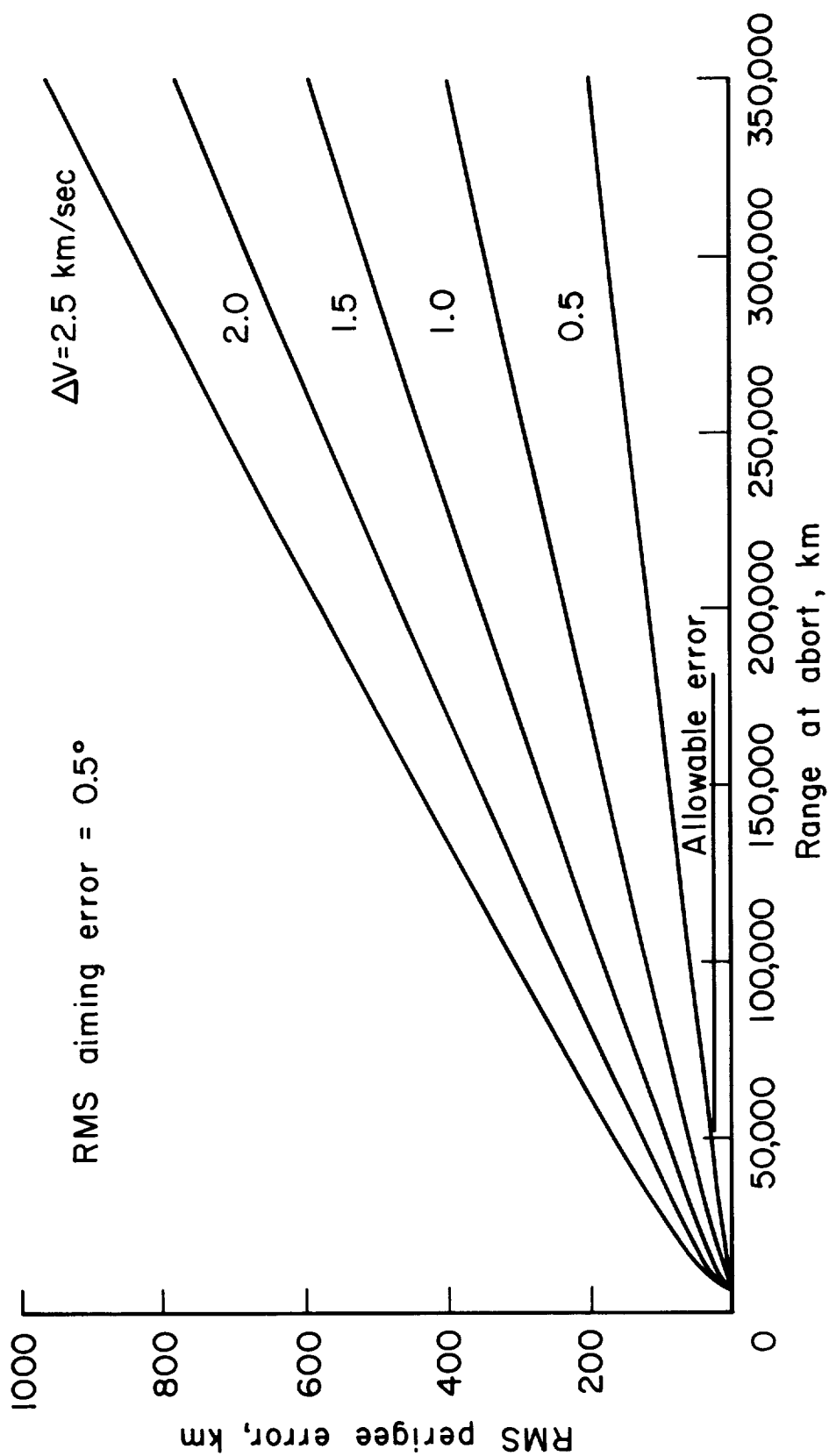
National Aeronautics and Space Administration.
Center, Moffett Field, Calif.
PREDICTION OF VELOCITY REQUIREMENTS FOR MINIMUM TIME ABORTS
FROM THE MIDCOURSE REGION OF A LUNAR MISSION

Robert B. Merrick and George P. Callas
Apr. 1963 40 p 7 refs
(NASA TN D-1655) OTS: \$1.00

5/2/63 1

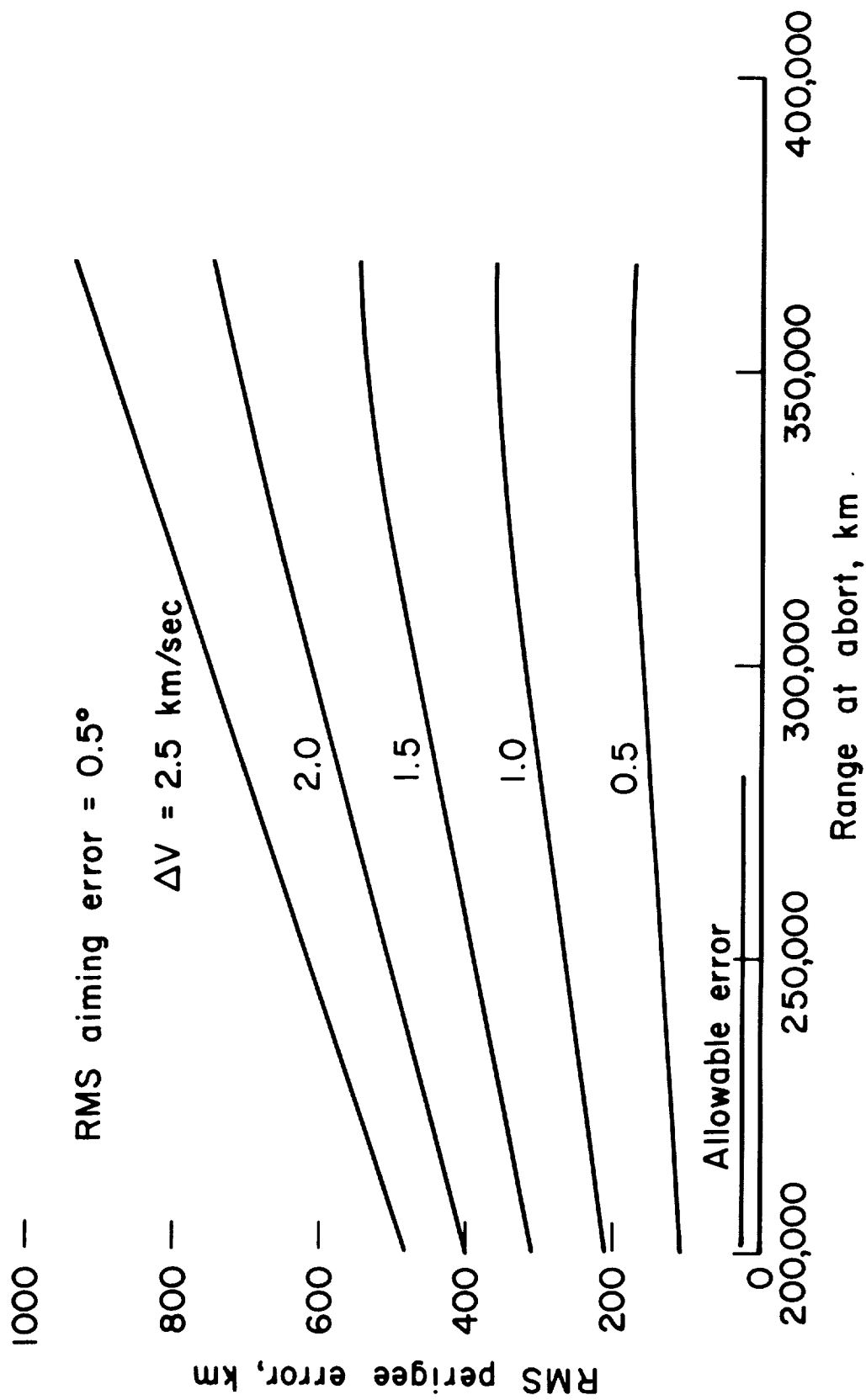
9 NASA-TN-D-1655
C-1 REPORT NO(S)
-
-
-





(a) Outbound leg.

Figure 8.- Perigee errors resulting from aiming errors.



(b) Return leg.

Figure 8.- Concluded.

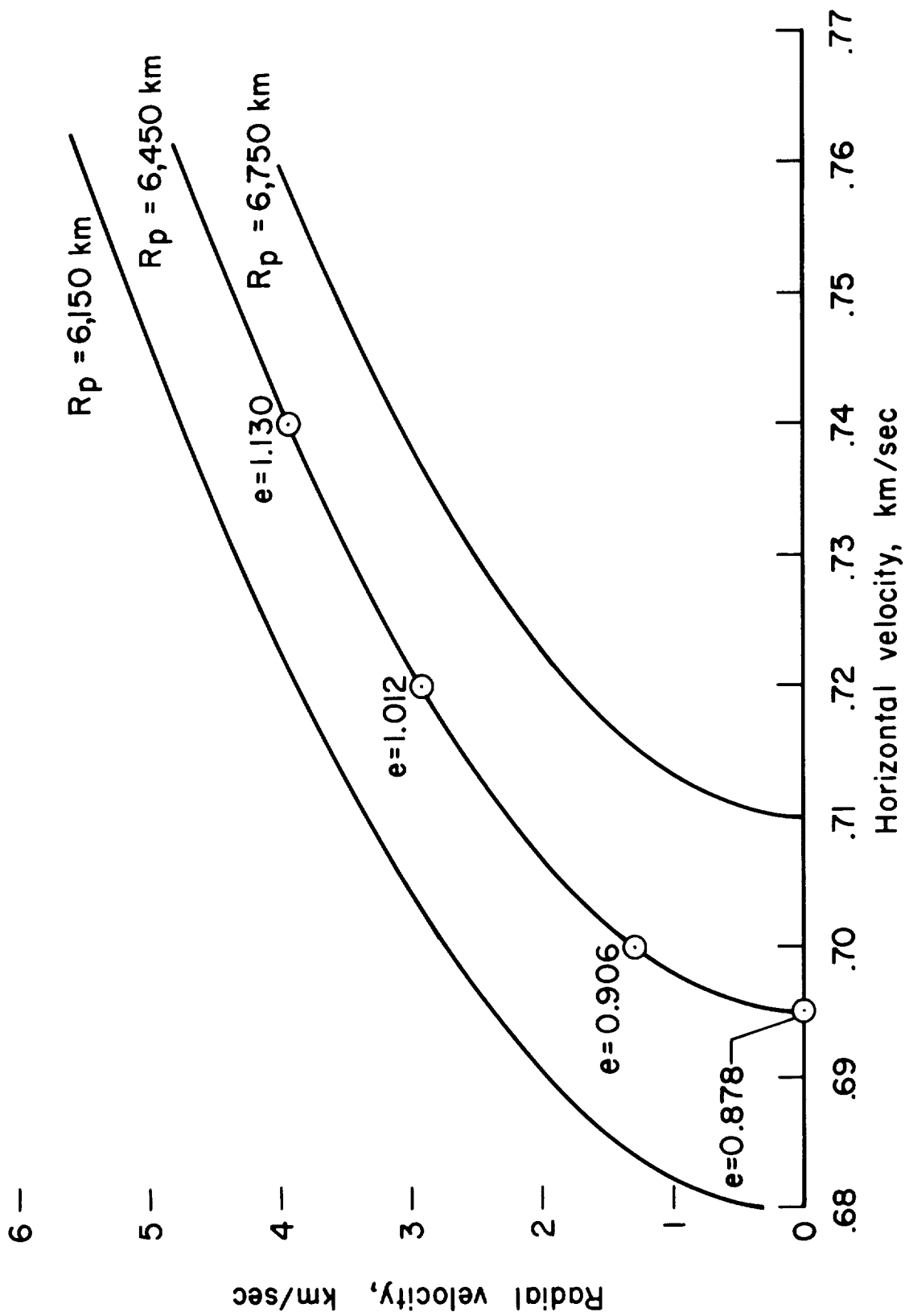


Figure 9.- Velocity increment required at a range of 100,000 km for correcting a 300 km perigee error.

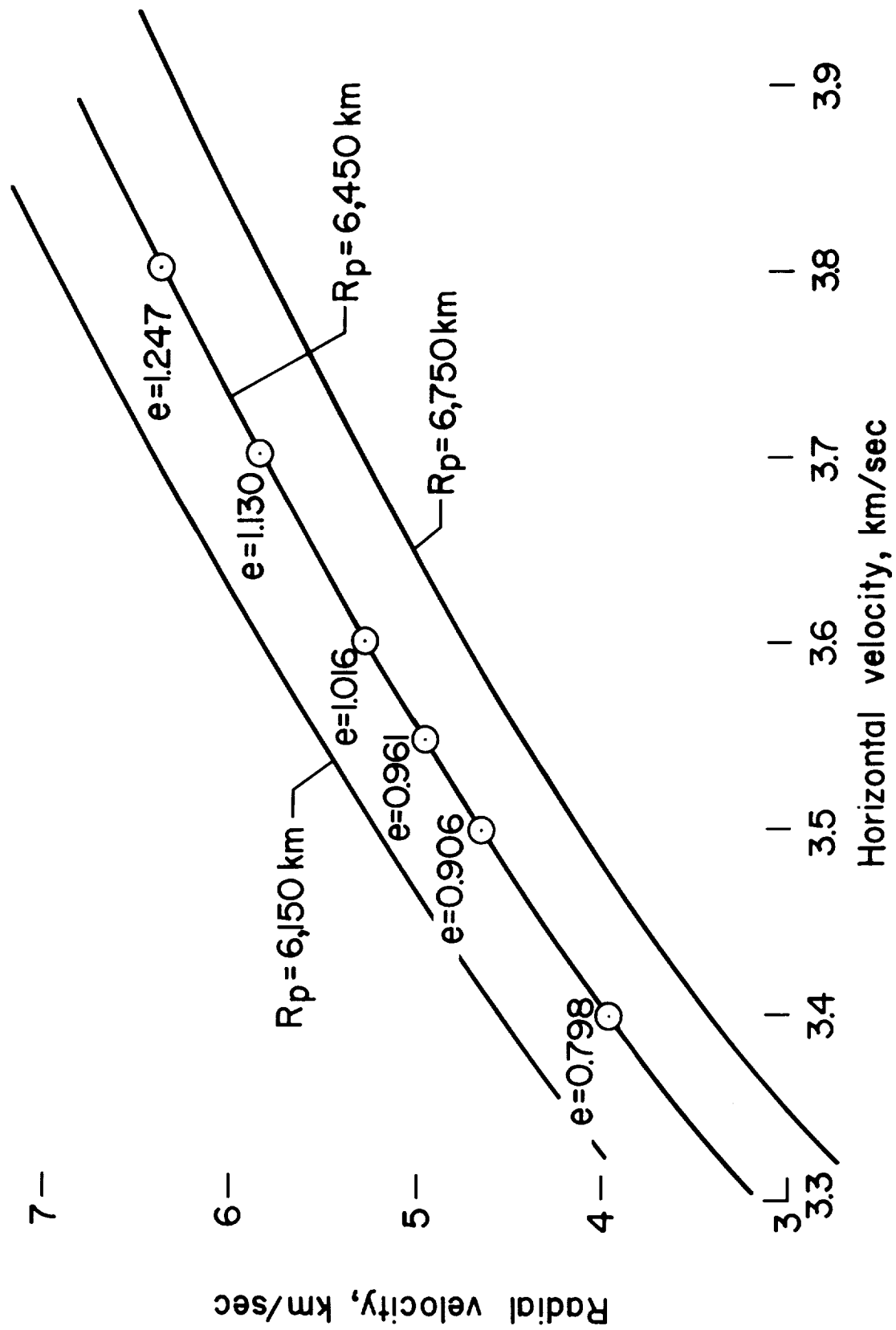


Figure 10.- Velocity increment required at a range of 20,000 km for correcting a 300 km perigee error.

